First satellite measurements of carbon dioxide and methane emission ratios in wildfire plumes

Adrian N. Ross,[1] Martin J. Wooster,[1] Hartmut Boesch,[2] and Robert Parker[2]

Received 29 May 2013; revised 3 July 2013; accepted 10 July 2013; published 2 August 2013.

[1] Using methane and carbon dioxide atmospheric mixing ratios retrieved using SWIR spectra from the Greenhouse Gases Observing SATellite (GOSAT), we report the first wildfire plume CH_4 to CO_2 emission ratios ($ER_{CH4/CO2}$) determined from space. We demonstrate the approach's potential using forward modeling and identify a series of real GOSAT spectra containing wildfire plumes. These show significantly changed total-column CO_2 and CH_4 mixing ratios, and from these we calculate $ER_{CH4/CO2}$ for boreal forest, tropical forest, and savanna fires as 0.00603, 0.00527, and 0.00395 mol mol^{-1}, respectively. These ERs are statistically significantly different from each other and from the "normal" atmospheric CH_4 to CO_2 ratio and generally agree with past ground and airborne studies. **Citation:** Ross, A. N., M. J. Wooster, H. Boesch, and R. Parker (2013), First satellite measurements of carbon dioxide and methane emission ratios in wildfire plumes, *Geophys. Res. Lett.*, *40*, 4098–4102, doi:10.1002/grl.50733.

1. Introduction

[2] Wildfires are one of the most important factors affecting atmospheric constituency, and accurate estimates of their emissions are critical to modeling many atmospheric chemistry and climate-related processes [*Andreae and Merlet*, 2001]. Emissions are usually estimated by multiplying the dry mass of vegetation burned by an emission factor EF_a, representing the amount of chemical species *a* released per kg of dry matter consumed. Biome-specific emissions factors (EFs) are widely published [e.g., *Yokelson et al*., 1999; *Wooster et al*., 2011] and intermittently summarized in global databases [e.g., *Andreae and Merlet*, 2001; *Akagi et al*., 2011]. With improving global estimates of amounts of vegetation consumed in wildfires, the accuracy of wildfire emissions estimates is increasingly limited by our knowledge of EFs [*van Leeuwen and van der Werf*, 2011; *Wooster et al*., 2011].

[3] Individual EFs are often determined using the carbon mass balance technique of *Ward and Radke* [1993], based on emission ratios of the target gas (*a*) in the smoke with respect to CO_2 ($ER_{a/CO2}$). Emission ratios themselves are generally based on excess mixing ratio measures (e.g., ΔX_a and ΔX_{CO2}) made during laboratory burns or field campaigns, but the former can be less representative of open landscape fires, and the latter biased towards easier-to-measure fires and often only at ground level [*van Leeuwen and van der Werf*, 2011; *Wooster et al*., 2011]. Airborne platforms [e.g., *Yokelson et al*., 1999] can alleviate some limitations, but can be costly and complex to deploy. An ability to derive ERs from spaceborne spectroscopy would thus offer many benefits, including measurement at remote locations and of intense burns and strongly-lofted plumes.

[4] Airborne and ground-based IR spectroscopy has been widely used to derive wildfire emissions ratios [e.g., *Yokelson et al*., 1999; *Wooster et al*., 2011], but only *Coheur et al*. [2009] and *Worden et al*. [2013] have derived them from spaceborne spectroscopy. Both used thermal IR (TIR) spectra, and in *Coheur et al*. [2009] wildfire ERs for ammonia (NH_3), ethene (C_2H_4), and methanol (CH_3OH) were determined with respect to carbon monoxide (CO). However, CO_2 and CH_4 were not retrieved despite being two of the main biomass-burning products, probably because the TIR spectrometer has little sensitivity to the boundary layer where many wildfire plumes remain.

[5] Retrievals of total column CO_2 and CH_4 mixing ratios from satellite remote sensing in clear skies are reasonably long-standing [e.g., *Kobayashi et al*., 1999], and the Greenhouse Gases Observing SATellite (GOSAT) has been designed to measure these using high-resolution SWIR spectroscopy with boundary layer sensitivity [*Buchwitz et al*., 2004]. Although aerosol-laden atmospheres can result in retrieval errors from GOSAT [e.g., *Boesche et al*., 2009], an "aerosol robust" scheme for methane based on the ratio of retrieved CH_4 and CO_2 columns has now been developed and applied to GOSAT [*Frankenberg et al*., 2005; *Parker et al*., 2011]. These developments make GOSAT a potential tool for the spaceborne measurement of wildfire CH_4 to CO_2 emission ratios, even in plumes with high aerosol loads. However, the sparse sampling pattern usually employed by GOSAT (see section 4) means that actually finding spectra containing wildfire plumes is challenging.

[6] In this study, we (i) assess the likely accuracy of GOSAT estimates of ΔX_{CO2}, ΔX_{CH4}, and $ER_{CH4/CO2}$ using forward modeling of SWIR spectra as observed in a range of atmospheres and "typical" wildfire plumes, (ii) describe the techniques developed to screen the GOSAT data archive for observations containing plumes, and (iii) use the knowledge gained to calculate the first wildfire $ER_{CH4/CO2}$ values using spaceborne measurements.

2. GOSAT Retrievals

[7] GOSAT was launched on 23 January 2009 carrying two main instruments: the "Thermal and Near Infrared Sensor for Carbon Observation Fourier-Transform Spectrometer" (TANSO-FTS) and the "TANSO Cloud and Aerosol Imager"

Additional supporting information may be found in the online version of this article.

[1]Department of Geography, King's College London, Strand, London, UK.
[2]Space Research Centre, University of Leicester, Leicester, UK.

Corresponding author: A. N. Ross, Department of Geography, King's College London, Strand, London WC2R 2LS, UK. (adrian.ross@kcl.ac.uk)

0094-8276/13/10.1002/grl.50733

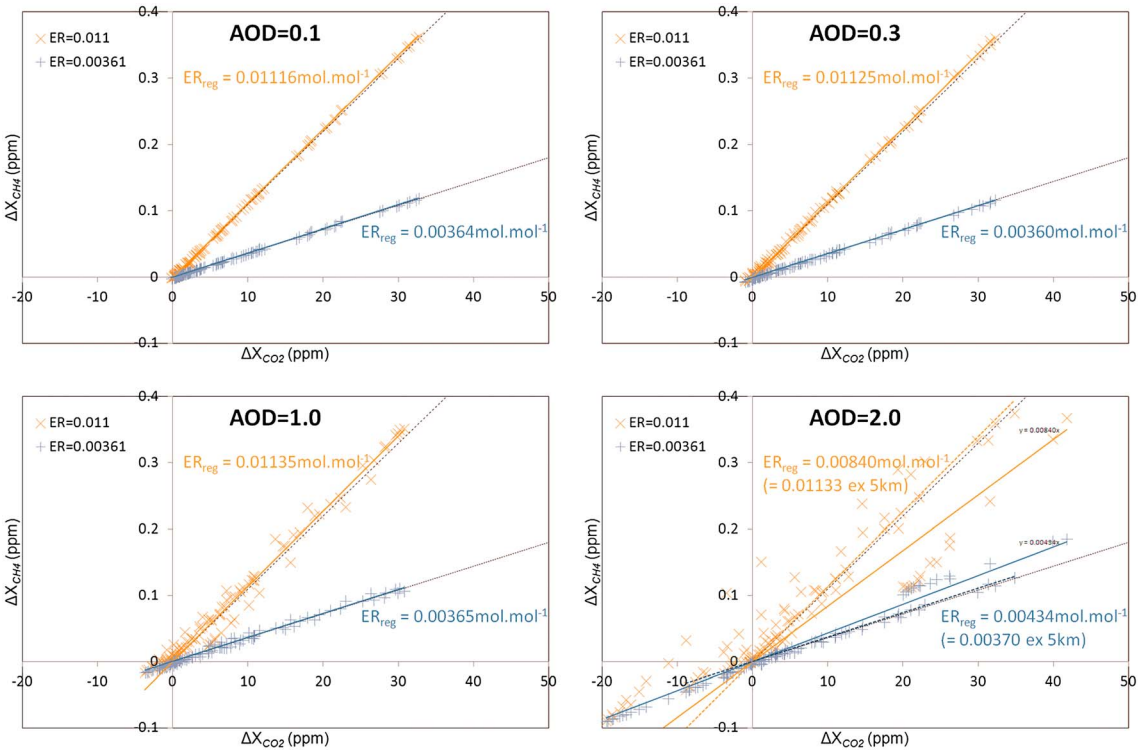

Figure 1. 2D scatterplots of the total column excess mixing ratio of methane (ΔX_{CH4}) against that of carbon dioxide (ΔX_{CO2}) as calculated from the retrievals from forward-modeled GOSAT TANSO-FTS spectra simulated using two different CH_4 to CO_2 emission ratios (0.011 for boreal forests plotted as blue and 0.00361 for savanna plotted as orange; values from *Akagi et al*. [2011]) for four AOD values (0.1, 0.3, 1.0, and 2.0). Least squares linear best fits to the two data sets are shown, along with dotted black lines showing the true emission ratios of 0.011 and 0.00361 used in the forward simulations. For simulations where AOD ≤ 1.0, the calculated emission ratios match those used in the forward modeling very well. For more opaque plumes (AOD = 2.0), the errors introduced by the thick aerosol layer remain significant, although when plumes with a height of 5 km are excluded, the calculated ratios again match the true ratios well (blue and orange dotted lines).

(TANSO-CAI) [*Hamazaki et al*., 2007]. TANSO-FTS operates in four bands: three in the SWIR (around 0.76, 1.6, and 2.0 μm); and one wide TIR band (5.5–14.3 μm), all with high (0.2 – 0.5 cm^{-1}) spectral resolution. The FTS field of view (FOV) has a ~10.5 km diameter, and in the high SNR observation pattern most commonly employed, three exposures are made at each point with ~260 km between points in either direction [*Kuze et al*., 2009]. TANSO-CAI is a four band imaging radiometer (0.380, 0.675, 0.870, and 1.600 μm) used to map cloud and aerosol characteristics [*Kuze et al*., 2009].

[8] We use retrieval results from the SWIR trace gas retrieval algorithm originally developed for retrieval of X_{CO2} from the NASA Orbiting Carbon Observatory (OCO) [*Boesch et al*., 2006, 2011], now modified to retrieve both X_{CO2} and X_{CH4} from TANSO-FTS SWIR spectra recorded over land [*Parker et al*., 2011; *Cogan et al*., 2012].

3. Simulations of GOSAT TANSO-FTS Spectra Affected by Wildfire Plumes

[9] To assess the potential of using GOSAT retrievals of X_{CO2} and X_{CH4} to infer $ER_{CH4/CO2}$ in the presence of wildfire plumes, we conducted forward modeling of SWIR spectra for a variety of plume situations. Five parameters were varied over ranges consistent with medium to large wildfires reported by other studies, notably *Kahn et al*. [2008], *Riggan et al*. [2004], and *Reid et al*. [2005]: plume height (0.3, 1, 2, and 5 km); plume vertical width (0.1 and 0.25, 0.5 and 1 km); maximum excess CO_2 at the plume center (10, 50,150, and 500 parts per million, ppm); aerosol optical depth at 0.76 μm (AOD; 0.1, 0.3, 1.0, and 2.0); and the proportion of black carbon in the aerosol (10% and 50%). Two different biomes were also simulated by using $ER_{CH4/CO2}$ values of 0.00361 mol mol^{-1} (savanna fires) and 0.011 mol mol^{-1} (boreal forest fires) [*Akagi et al*., 2011].

[10] From these scenarios, we built 1024 20-level atmospheric profiles by assuming excess CO_2, CH_4, and smoke aerosols were normally distributed vertically around the plume's mean height, with a standard deviation of half the plume width. We also filtered out results where plume width equalled or exceeded 0.5 km and excess CO_2 was 500 ppm, since this situation is unlikely in reality. The resulting atmospheric profiles were used with the OCO retrieval algorithm's forward model to generate SWIR spectral radiances, spectrally degraded to simulate TANSO-FTS observations. We processed the simulated spectra through the GOSAT retrieval algorithm to retrieve CO_2 and CH_4 columns, together with a multiplicative scale factor for the water vapor profile, an additive shift to the temperature profile, the surface albedo, and its spectral slope. The *a priori* for the atmospheric CO_2 and CH_4 profile was taken as the unperturbed (no plume) case, and no aerosol was included in the retrieval. For surface pressure, we use values inferred from the O_2 A-Band [*Parker et al*., 2011].

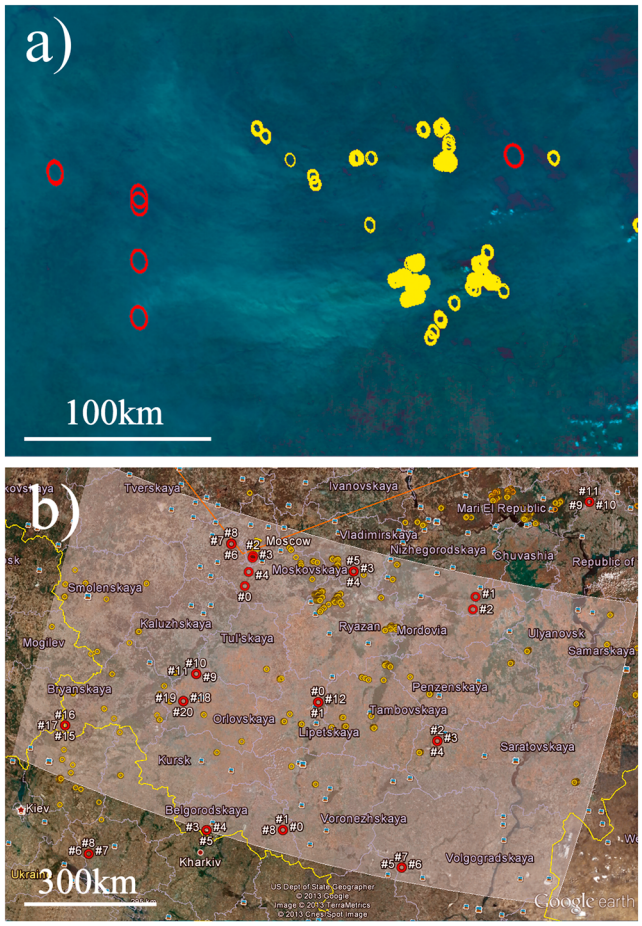

Figure 2. Example images from techniques used to aid identification of FTS smoke plume exposures, showing wildfires to the east of Moscow (main cluster around 55.13°N, 39.93° E) on 8 August 2010. (a) Subset of the wide-area locator image produced from CAI file GOSATTCAI20100808105001802 20_1BTRB0V00900.h5 (rendered with RGB = CAI bands 4, 3, and 1, respectively), with the 10.5 km diameter FTS FOVs bounded by the red ellipses and active fire locations from the closest matching MODIS MYD14 active fire product marked by yellow ellipses. (b) View of the entire CAI scene plotted as a Google Earth kml file, with CAI extent marked approximately by the white area, FTS FOVs marked by red circles (not to scale), and active fire locations marked by yellow circles.

[11] We compared "retrieved" ΔX_{CO2} and ΔX_{CH4} to the "true" values from the simulations (see electronic appendix). For low aerosol loads (AOD ≤ 0.3), the retrievals reproduced "truth" very well (e.g., 95% of ΔX_{CO2} retrievals lie within 1.2 ppm of truth). For AOD = 1, errors increase somewhat (95% within 4.6 ppm), and when AOD = 2 become much more significant (95% within 21.4 ppm). Although the errors in the most aerosol-laden plumes appear rather large, because the GOSAT CO_2 and CH_4 retrievals are made at very similar wavelengths (1.61 μm and 1.65 μm), the aerosol impacts and resulting errors are actually very similar for both gases [*Butz et al*., 2010], thus tending to cancel out in the ratio-based $ER_{CH4/CO2}$ calculation. Plotting ΔX_{CH4} against ΔX_{CO2} to determine $ER_{CH4/CO}$ (as per *Yokelson et al*. [1999]) for different AOD values therefore provides a retrieved $ER_{CH4/CO2}$ very close to the true $ER_{CH4/CO2}$ used in the simulations, at least where AOD ≤ 1 (all results within 2.7%, Figure 1). For AOD = 2, the ratios do differ substantially, but excluding simulations with the highest plumes (>5 km) brings the retrieved $ER_{CH4/CO2}$ into good agreement with the true values (shown by dotted lines in Figure 1). Few wildfire smoke plumes reach 5 km altitude [*Kahn et al*., 2008], and few show 0.76 μm AOD >> 1 far downwind of fires where the TANSO-FTS footprint typically falls [*Eck et al*., 2003], so we conclude that it may be possible to determine $ER_{CH4/CO2}$ from wildfire-plume TANSO-FTS spectra with reasonable accuracy.

[12] Modeling also suggests that, since satellite-derived ERs are based on total-column excess amounts rather than point-based measures, they may be less sensitive to errors introduced by mixing between different ambient air masses [*Yokelson et al*., 2013].

4. Identifying FTS Exposures Containing Wildfire Smoke Plumes

[13] We obtained TANSO-FTS and -CAI Level 1B data from the GOSAT User Interface Gateway, but since FTS observes only ~0.2% of Earth's surface every three-day repeat cycle actually finding exposures containing wildfire plumes is challenging. To aid efficiency, but still sample the key wildfire biomes of *Akagi et al*. [2011], we limited our search to the 2009–2011 annual fire seasons in northern and southern Africa and Australia ("savanna"), Amazonia and Indonesia ("tropical forest") and Canada and the unusually large 2010 Russian wildfires ("boreal forest").

[14] We first plotted each FTS FOV on a matching "wide-area locator" CAI color composite (RGB = bands 4, 3, and 1) to gauge whether it contained wildfire smoke or cloud (Figure 2a). Although smaller CAI-based "locator images" are already available for some FTS L1B data, they only show the area immediately surrounding the FTS FOV, making it slow to classify multiple exposures and hard to assess whether wildfires are the source of observed aerosols.

[15] To further aid confident plume identification, we overlaid the matching MODIS MYD14 active fire locations [*Justice et al*., 2002] on the CAI scene (Figure 2a). We also output daily locations of the CAI scenes, FTS exposures, and MODIS active fires as KML files, enabling "Google Earth" to be used to identify dates and locations where FTS FOVs lie close to wildfires without needing to download and review every 120 megabyte CAI data set (Figure 2b).

[16] Finally, TANSO-FTS plume observations identified early on indicated that nearly all showed the characteristics of elevated ammonia mixing ratios (X_{NH3}) in the TIR spectra. Therefore, in an approach similar to *Clarisse et al*. [2009], we used a simple three-point brightness temperature measure (ΔBT_{NH3}) around the ammonia absorption band to identify exposures likely to contain wildfire smoke (see electronic appendix). Clouds can also produce elevated ΔBT_{NH3}, so it was still necessary to actually view the CAI scene to confirm the cause as smoke, but this enabled large numbers of FTS exposures to be assessed rapidly without reviewing all CAI scenes.

[17] Using these methods, we identified a set of obvious "smoke plume" FTS exposures for Canada, Russia, and the Amazon. We found no such obvious exposures in Africa, Australia, or Indonesia, in the latter case possibly due to the

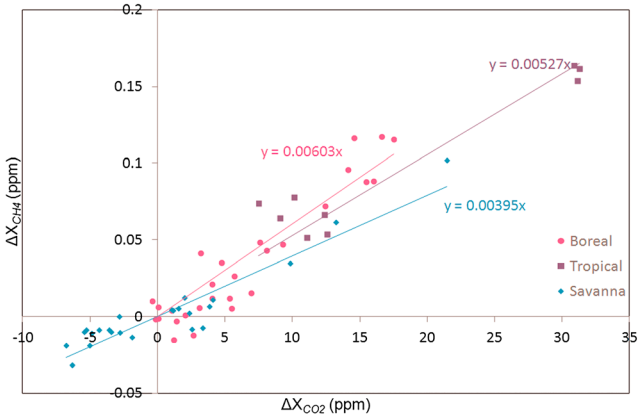

Figure 3. Total-column excess mixing ratio of methane (ΔX_{CH4}) plotted against that of CO_2 (ΔX_{CO2}) for the 61 "smoke-plume" TANSO-FTS exposures for which CO_2 and CH_4 concentrations were successfully retrieved, grouped by biome (boreal forest, tropical forest and savanna). The gradients of the three least squares linear best fits (forced through the origin) represent the biome-specific emission ratios ($ER_{CH4/CO2}$). Fit uncertainties are reported in the main text and electronic appendix.

relatively small land area that reduced the number of relevant FTS observations. In Africa and Australia, we attribute this to the lower fuel load of savannas, and the fact that savanna burns often produce less visible plumes with lower aerosol amounts. However, for Africa, we were able to identify exposures having both elevated ΔBT_{NH3} and lying downwind of fires, even though plumes were not clearly visible in the wide-area locator images. We therefore included these in our smoke plume exposure data set.

[18] To these exposures we applied the retrieval scheme of *Parker et al.* [2011] for X_{CO2} and X_{CH4}, using versions 050050, 080080, 100100, and 110110 of the FTS spectra and v3.2 of the aerosol robust retrieval algorithm, including results that would normally be excluded as "cloudy" based on a comparison of surface pressure derived from the O2 A-Band and the ECMWF surface pressure interpolated to the measurement time and location. Finally, we calculated ΔX_{CH4} and ΔX_{CO2} by subtracting the X_{CO2} and X_{CH4} retrievals from a nearby (geographically and temporally) cloud- and smoke-free "control exposure" that had converging retrievals, and with X_{CO2} and X_{CH4} within 0.5 standard deviations of the mean for the area and season.

5. Results and Discussion

[19] From a total of 123,218 TANSO-FTS spectra, the above screening identified 114 smoke plume exposures. Part of a wide-area locator image for one of these is shown in Figure 2a, and the complete list is included in the electronic appendix. Of the 114, 36 failed retrieval tests of signal-to-noise and data quality (χ^2), and 17 more contained cloud and were discounted. This left 61 smoke plume exposures for our final derivation of $ER_{CH4/CO2}$: 28 boreal forest; 9 tropical forest; and 24 savanna.

[20] Every smoke plume exposure lay tens to hundreds of km downwind of the fire itself, and most showed positive ΔX_{CO2} and ΔX_{CH4}, including values in excess of +30 ppm for CO_2 and +0.15 ppm for CH_4 (Figure 3). Although other studies report wildfire plume ΔX_{CO2} of hundreds or even thousands of ppm [e.g., *Riggan et al.*, 2004; *Wooster et al.*, 2011], these relate to point-based or short-path measures relatively close to the fire source, not the column averages that GOSAT provides in which the smoke plume represents only a relatively small portion. A small number of exposures show negative ΔX_{CO2} and ΔX_{CH4}, mostly in the savanna biome and probably because some do not actually contain wildfire plumes (see section 4). Also, our simulations already indicated that some plume situations can result in apparently negative excess mixing ratios (Figure 1).

[21] From the data of Figure 3, we infer wildfire $ER_{CH4/CO2}$ values of 0.00603 ± 0.00033, 0.00527 ± 0.00029, and 0.00395 ± 0.00029 mol mol^{-1} for boreal forest, tropical forest and savanna biomes respectively. All ERs are highly statistically significant (significance $p < 4.7\times10^{-6}$ and $0.93 \le R^2 \le 0.97$) and are also all statistically significantly different from the "normal atmosphere" X_{CH4}/X_{CO2} ratio ($p < 0.034$) and from one another, except for the difference between ER_{Boreal} and $ER_{Tropical}$ ($p = 0.188$).

[22] The biome-specific $ER_{CH4/CO2}$ values determined here lie within the ranges reported in *Akagi et al.* [2011] (0.01101 ± 0.00580, 0.00849 ± 0.00331, and 0.00316 ± 0.00139 mol mol^{-1}, respectively) and in the same rank order ($ER_{Boreal} > ER_{Tropical} >$ "clean atmosphere" $> ER_{Savanna}$). However, $ER_{CH4/CO2}$ differences between the biomes are less pronounced than between the median values of *Akagi et al.* [2011], possibly because in these large wildfires the fuel types are more mixed than in the smaller-scale burns included in most EF databases.

6. Summary and Conclusion

[23] Using simulations and actual retrievals, we have confirmed the potential of the GOSAT spectrometer to measure atmospheric trace gas increases in individual wildfire plumes, albeit with some errors introduced by smoke aerosols. We have also shown that, because of the proximity of the CO_2 and CH_4 retrieval wavelengths, these retrievals can be used to calculate $ER_{CH4/CO2}$ accurately in most situations.

[24] We have identified TANSO-FTS exposures containing wildfire plumes across three key biomes, have observed altered CO_2 and CH_4 mixing ratios in these exposures, and have derived biomass-burning CH_4 to CO_2 emission ratios (we believe for the first time using spaceborne spectroscopy). The use of CO_2 as the reference gas is important, as knowledge of ERs with respect to CO_2 is preferable for the calculation of the EFs necessary to convert wildfire fuel consumption into emissions' estimates [*Ward and Radke*, 1993].

[25] Our ERs calculated for boreal forest, tropical forest and savanna fires lie within the ranges reported by prior studies. We therefore conclude that this technique offers promise for improving knowledge of wildfire emission ratios, especially if future spaceborne spectrometers have narrowed FOVs and an ability to target wildfire plumes specifically.

[26] **Acknowledgments.** We thank JAXA, NIES, and MOE for GOSAT data and their support as part of the Joint Research Agreement. R.P. and M.J.W are supported by the NERC National Centre for Earth Observation (NCEO). R.P. is also supported by the ESA Climate Change Initiative, and M.J.W by the EU Seventh Research Framework Programme (MACC-II project, contract 283576). We also thank BADC for providing ECMWF Operational Analyses data used in retrievals.

[27] The Editor thanks two anonymous reviewers for their assistance in evaluating this paper.

References

Akagi, S. K., R. J. Yokelson, C. Wiedinmyer, M. J. Alvarado, J. S. Reid, T. Karl, J. D. Crounse, and P. O. Wennberg (2011), Emission factors for open and domestic biomass burning for use in atmospheric models, *Atmos. Chem. Phys.*, *11*, 4039–4072.

Andreae, M. O., and P. Merlet (2001), Emission of trace gases and aerosols from biomass burning, *Global Biogeochem. Cycles*, *15*, 955–966.

Boesch, H., et al. (2006), Space-based near-infrared CO2 measurements: Testing the Orbiting Carbon Observatory retrieval algorithm and validation concept using SCIAMACHY observations over Park Falls, Wisconsin, *J. Geophys. Res.*, *111*, D23302, doi:10.1029/2006JD007080.

Boesch, H., D. Baker, B. Connor, D. Crisp, and C. Miller (2011), Global characterization of CO2 column retrievals from shortwave-infrared satellite observations of the Orbiting Carbon Observatory-2 mission, *Remote Sens.*, *3*(2), 270–304.

Boesche, E., P. Stammes, and R. Bennartz (2009), Aerosol influence on polarization and intensity in near-infrared O2 and CO2 absorption bands observed from space, *J. Quant. Spectrosc. Ra.*, *110*, 223–239.

Buchwitz, M., et al. (2004), Atmospheric methane and carbon dioxide from SCIAMACHY satellite data: initial comparison with chemistry and transport models, *Atmos. Chem. Phys. Discuss.*, *4*, 7217–7279.

Butz, A., O. P. Hasekamp, C. Frankenberg, J. Vidot, and I. Aben (2010), CH4 retrievals from space-based solar backscatter measurements: Performance evaluation against simulated aerosol and cirrus loaded scenes, *J. Geophys. Res.*, *115*, D24302, doi:10.1029/2010JD014514.

Clarisse, L., C. Clerbaux, F. Dentener, D. Hurtmans, and P.-F. Coheur (2009), Global ammonia distribution derived from infrared satellite observations, *Nat. Geosci.*, *2*, 479–483.

Cogan, A., et al. (2012), Atmospheric carbon dioxide retrieved from the Greenhouse gases Observing SATellite (GOSAT): Comparison with ground-based TCCON observations and GEOS-Chem model calculations. *J. Geophys. Res.*, *117*, D21301, doi:10.1029/2012JD018087.

Coheur, P.-F., L. Clarisse, S. Turquety, D. Hurtmans, and C. Clerbaux (2009), IASI measurements of reactive trace species in biomass burning plumes, *Atmos. Chem. Phys.*, *9*, 5655–5667.

Eck, T. F., B. N. Holben, J. S. Reid, N. T. O'Neill, J. S. Schafer, O. Dubovik, A. Smirnov, M. A. Yamasoe, and P. Artaxo (2003), High aerosol optical depth biomass burning events: A comparison of optical properties for different source regions, *Geophys. Res. Lett.*, *30*, 2035, doi:10.1029/2003GL017861.

Frankenberg, C., J. F. Meirink, M. van Weele, U. Platt, and T. Wagner (2005), Assessing methane emissions from global spaceborne observations, *Science*, *308*, 1010–1014, doi:10.1126/science.1106644.

Hamazaki, T., Y. Kaneko, A. Kuze, and H. Suto (2007), Greenhouse gases observation from space with TANSO-FTS on GOSAT, presented at the Fourier Transform Spectroscopy / Hyperspectral Imaging Sounding Environment, Santa Fe, NM, 2007, Paper FWB1.

Justice, C. O., L. Giglio, S. Korontzi, J. Owens, J. Morisette, D. Roy, J. Descloitres, S. Alleaume, F. Petitcolin, and Y. Kaufman (2002), The MODIS fire products, *Remote Sens. Environ.*, *83*, 244–262.

Kahn, R. A., Y. Chen, D. L. Nelson, F.-Y. Leung, Q. Li, D. J. Diner, and J. A. Logan. (2008), Wildfire smoke injection heights: Two perspectives from space, *Geophys. Res. Lett.*, *35*, L04809, doi:10.1029/2007GL032165.

Kobayashi, H., A. Shimota, K. Kondo, E. Okumura, Y. Kameda, H. Shimoda, and T. Ogawa (1999), Development and evaluation of the interferometric monitor for greenhouse gases: a high-throughput Fourier-transform infrared radiometer for nadir Earth observation, *Appl. Optics*, *38*, 6801–6807.

Kuze, A., H. Suto, M. Nakajima, and T. Hamazaki (2009), Thermal and near infrared sensor for carbon observation Fourier-transform spectrometer on the Greenhouse Gases Observing Satellite for greenhouse gases monitoring, *Appl. Optics*, *48*(35), 6716–6733.

Parker, R., et al. (2011), Methane observations from the Greenhouse Gases Observing SATellite: Comparison to ground-based TCCON data and model calculations, *Geophys. Res. Lett.*, *38*, L15807, doi:10.1029/2011GL047871.

Reid, J. S., R. Koppmann, T. F. Eck, and D. P. Eleuterio (2005), A review of biomass burning emissions part II: intensive physical properties of biomass burning particles, *Atmos. Chem. Phys.*, *5*, 799–825.

Riggan, P. J., R. G. Tissell, R. N. Lockwood, J. A. Brass, J. A. R. Pereira, H. S. Miranda, A. C. Miranda, T. Campos, and R. Higgins (2004), Remote measurement of energy and carbon flux from wildfires in Brazil, *Ecol. Appl.*, *14*, 855–872.

van Leeuwen, T. T., and G. R. van der Werf (2011), Spatial and temporal variability in the ratio of trace gases emitted from biomass burning, *Atmos. Chem. Phys.*, *11*, 3611–3629.

Ward, D. E., and L. F. Radke (1993), Emissions measurements from vegetation fires: A comparative evaluation of methods and results, in *Fire in the Environment: The Ecological, Atmospheric and Climatic Importance of Vegetation Fires*, edited by P. J. Crutzen, and J. G. Goldammer, pp. 53–76, John Wiley, New York.

Wooster, M. J., P. H. Freeborn, S. Archibald, C. Oppenheimer, G. J. Roberts, T. E. L. Smith, N. Govender, M. Burton, and I. Palumbo (2011), Field determination of biomass burning emission ratios and factors via open-path FTIR spectroscopy and fire radiative power assessment: Headfire, backfire and residual smouldering combustion in African savannahs, *Atmos. Chem. Phys. Discuss.*, *11*, 3259–3578.

Worden, J., K. Wecht, C. Frankenberg, M. Alvarado, K. Bowman, E. Kort, S. Kulawik, M. Lee, V. Payne, and H. Worden (2013), CH4 and CO distributions over tropical fires during October 2006 as observed by the Aura TES satellite instrument and modeled by GEOS-Chem, *Atmos. Chem. Phys.*, *13*, 3679–3692.

Yokelson, R. J., J. G. Goode, D. E. Ward, R. A. Susott, R. E. Babbitt, D. D. Wade, I. Bertschi, D. W. T. Griffith, and W. M. Hao (1999), Emissions of formaldehyde, acetic acid, methanol, and other trace gases from biomass fires in North Carolina measured by airborne Fourier transform infrared spectroscopy, *J. Geophys. Res.*, *104*, 30,109–30,125.

Yokelson, R. J., M. O. Andreae, and S. K. Akagi (2013), Pitfalls with the use of enhancement ratios or normalized excess mixing ratios measured in plumes to characterize pollution sources and aging, *Atmos. Meas. Tech. Discuss.*, *6*, 4077–4085.